Characterization of Cu-ZSM-5 Prepared by Solid-State Ion Exchange of H-ZSM-5 with CuCl

Yihua Zhang, Ian J. Drake, and Alexis T. Bell*

Department of Chemical Engineering, University of California, Berkeley, California 94720-1462

Received October 17, 2005. Revised Manuscript Received March 2, 2006

The solid-state ion exchange (SSIE) of H-ZSM-5 by CuCl vapor was investigated with the objective of establishing the effects of the temperature at which exchange is carried out on the level of proton exchange for Cu^+, the position of the Cu^+ cations relative to the zeolite lattice, and the extent of CuCl occlusion in the zeolite pores. After SSIE, the resulting Cu-ZSM-5 was characterized by XRD, ^{27}Al MAS NMR, infrared spectroscopy, H_2-TPR, and Cu and Cl K-edge X-ray absorption spectroscopy. Evidence was found for clusters of CuCl, in addition to Cu^+ cations present at zeolite cation-exchange positions (ZCu). It was also observed that a part of the occluded CuCl is hydrolyzed to Cu_2O during SSIE. The distribution of ZCu, CuCl, and Cu_2O was a strong function of the temperature at which cation exchange was carried out. Virtually complete exchange of all Brønsted acid protons for Cu^+ cations was achieved at a SSIE temperature of 1023 K. No loss of framework Al was observed at this temperature, and only 10% of the copper introduced into the zeolite was occluded as CuCl. The Cu^+ cations exchanged for Brønsted acid protons are both doubly and triply coordinated to O atoms, with an average Cu−O bond distance of 1.98 Å. Cu EXAFS and Cl XANES indicated that CuCl is occluded in the form of $(CuCl)_n$ ($n = 2, 3, 4$) clusters in the channels and intersections of the zeolite. With a decrease in the amount of occluded CuCl, the amount of Cu_2O formed by hydrolysis during SSIE decreases substantially.

Introduction

Cu-ZSM-5 is an active catalyst for the decomposition of NO to N_2 and O_2,[1−13] the synthesis of methanol,[14] the conversion of 1-propanamine to C_6 imines and nitriles,[15] the desulfurization of diesel fuel,[16] and the oxidative carbonylation of methanol to dimethyl carbonate.[17] Moreover, infrared studies and quantum chemical calculations suggest that Cu-ZSM-5 can activate double and triple bonds in alkenes, alkynes, and other electron-rich molecules (e.g., benzene and acetone).[18] The broad range of reactions catalyzed by Cu-ZSM-5 has stimulated efforts to understand the effects of catalyst preparation on the local structure and oxidation state of the Cu cations present within the zeolite. A closely related goal has been the preparation of Cu-ZSM-5 in which all of the charge-exchange sites are occupied by Cu cations. Characterization of Cu-ZSM-5 prepared by conventional aqueous exchange of Na-ZSM-5 with solutions of $CuCl_2$, $Cu(NO_3)_2$, or $Cu(CH_3COO)_2$ has shown that the maximum exchange level is Cu/Al ≈ 0.5 and that the Cu^{2+} cations can be present as either isolated cations or copper-oxo clusters.[4,9−13,19−26] While attempts have been made to carry out aqueous exchange using a solution containing Cu^+

* To whom correspondence should be addressed. Tel: 510-642-1536. Fax: 510-642-4778. E-mail: bell@cchem.berkeley.edu.

(1) Iwamoto, M.; Yahiro, H.; Tanada, K.; Mozino, Y.; Kagawa, S. *J. Phys. Chem.* **1991**, *95*, 3727. Shelef, M. *Chem. Rev.* **1995**, *95*, 209.
(2) Smits, H. H. R.; Iwasawa, Y. *Appl. Catal. B* **1995**, *6*, 201.
(3) Hamada, H.; Matsubayashi, N.; Shimada, H.; Kintaichi, Y.; Ito, T.; Nishijima, A. *Catal. Lett.* **1990**, *5*, 291.
(4) Larsen, S.; Aylor, A.; Bell, A. T.; Reimer, J. *J. Phys. Chem.* **1994**, *98*, 11533. Hu, S.; Reimer, J.; Bell, A. T. *J. Phys. Chem. B* **1997**, *101*, 1869.
(5) Li, Y.; Hall, W. K. *J. Catal.* **1991**, *129*, 202.
(6) Beutel, T.; Sarkany, J.; Lei, G. D.; Yan, J. Y.; Sachtler, W. M. H. *J. Phys. Chem.* **1996**, *100*, 845.
(7) Moretti, G.; Ferraris, G.; Fierro, G.; Lo Jacono, M.; Morpurgo, S.; Faticanti, M. *J. Catal.* **2005**, *232*, 476.
(8) Praserthdam, P.; Isarangura na Ayutthaya, S. *Catal. Today* **2004**, *97*, 137.
(9) Groothaert, M. H.; Lievens, K.; Leeman, H.; Weckhuysen, B. M.; Schoonheydt, R. A. *J. Catal.* **2003**, *220*, 500.
(10) Kuroda, Y.; Yagi, K.; Horiguchi, N.; Yoshikawa, Y.; Kumashiro, R.; Nagao, M. *Phys. Chem. Chem. Phys.* **2003**, *5*, 3318.
(11) Fanson, P. T.; Stradt, M. W.; Lauterbach, J.; Delgass, W. N. *Appl. Catal. B* **2002**, *38*, 331.
(12) Da Costa, P.; Moden, B.; Meitzner, D. G.; Lee K. D.; Iglesia E. *Phys. Chem. Chem. Phys.* **2002**, *4*, 4590.
(13) Turnes Palomino, G.; Fisicaro, P.; Bordiga, S.; Zecchina, A.; Giamello, E.; Lamberti, C. *J. Phys. Chem. B* **2000**, *104*, 4064.
(14) Chen, H. Y.; Chen, L.; Lin, J.; Tan, K. L.; Li, J. *Inorg. Chem.* **1997**, *36*, 1417.
(15) Kanazirev, V. I.; Price, G. L.; Dooley, K. M. *J. Catal.* **1994**, *148*, 164. Guidry, T. F.; Price, G. L. In *Catalysis of Organic Reactions*; Herkes, F. E., Ed.; Marcel Dekker: New York, 1998; p 601. Guidry T. F.; Price, L. G. *J. Catal.* **1999**, *181*, 16.
(16) Hernandez-Maldonado, A. J.; Yang, R. T. *AIChE J.* **2004**, *50*, 791.
(17) Anderson, S. A.; Root, T. W. *J. Mol. Catal. A* **2004**, *220*, 247.
(18) Broclawik, E.; Kozyra, P.; Datka, J. *C. R. Chim.* **2005**, *8*, 491.
(19) Kuroda, Y.; Kumashiro, R.; Itadani, A.; Nagao, M.; Kobayashi, H. *Phys. Chem. Chem. Phys.* **2001**, *3*, 1383.
(20) Bulánek, R.; Wichterlová, B.; Sobalík, Z.; Tich×c6, J. *Appl. Catal. B* **2001**, *31*, 13.
(21) Aylor W. A.; Larsen C. S.; Reimer, A. J.; Bell, T. A. *J. Catal.* **1995**, *157*, 592.
(22) Neylon, M. K.; Marshall, C. L.; Kropf, A. J. *J. Am. Chem. Soc.* **2002**, *124*, 5457.
(23) Castagnola, N. B.; Knopf, A. J.; Marshall, C. L. *Appl. Catal. A* **2005**, *290*, 110.
(24) Tkachenko, O. P.; Klementiev, K. V.; Koc, N.; Yu, X.; Bandyopadhyay, M.; Woll, C.; Grabowski, S.; Gies, H.; Grunert, W. *Stud. Surf. Sci. Catal.* **2004**, *154*, 1670.
(25) Tkachenko, O. P.; Klementiev, K. V.; van den Berg, M. W. E.; Koc, N.; Bandyopadhyay, M.; Birkner, A.; Woll, C.; Gies, H.; Grunert. *J. Phys. Chem. B* **2005**, *109*, 20979.
(26) Bolis, V.; Barbaglia, A.; Bordiga, S.; Lamberti, C.; Zecchina, A. *J. Phys. Chem. B* **2004**, *108*, 9970.

10.1021/cm052291m CCC: $33.50
Published on Web 04/07/2006

cations, exchange levels above 0.5 could not be achieved.[27] Higher exchange levels by Cu^+ cations can be attained by solid-state ion exchange (SSIE), and a significant number of studies have been devoted to characterizing Cu-ZSM-5 produced by this means.

Zecchina and co-workers[26,28−40] have reported that the protons in H-ZSM-5 are exchanged quantitatively for Cu^+ cations when the zeolite is contacted with CuCl vapor at either 573 or 673 K and then heated in a vacuum at 773 K to remove excess CuCl. XANES and EXAFS characterization of the resulting Cu-ZSM-5 reveal that all of the Cu is present as Cu^+ and that the average Cu−O coordination number and bond distance are 2.5 and 2.00 Å, respectively. Kuroda et al.[10] have also used the SSIE technique to prepare Cu-ZSM-5. From infrared spectra of the O−H stretching region, they inferred that after SSIE at 573 K some CuCl remained associated with the Brønsted acid protons and that completion of the reaction between CuCl and Brønsted acid protons did not occur until the zeolite was heated in vaccum at 623 K. Characterization of Cu-ZSM-5 after SSIE showed that all of the Cu was present as Cu^+ and that the Cu−O bond distance was 2.10 Å.

While SSIE can be used to obtain high levels of Cu^+ exchange for proton, the question of whether CuCl is occluded in the zeolite and the extent to which it can be removed by thermal treatment has been examined to only a limited degree. Li et al.[41] have observed that CuCl sublimes easily and disperses on the surface of the zeolite. The reaction of CuCl with the protons of H-Y occurred above 573 K, and the maximum level of exchange was achieved at 613 K. XRD revealed that crystalline CuCl could still be observed after treatment of the CuCl/H-Y sample at 623 K for 60 h or 823 K for 5 h. More recently, Drake et al.[42,43] have investigated the SSIE of H-USY, H-Y, and H-ZSM5 with CuCl. These studies showed that depending on the conditions of exchange up to 40% of the Cu introduced into the zeolite was either CuCl or $Cu(OH)_3Cl$. Therefore, it is clear that the occlusion of CuCl in the zeolite pores needs to be considered carefully and conditions established for its minimization.

In this paper, we report the results of a detailed study aimed at gaining insight into the interaction between CuCl and H-ZSM-5 zeolite as a function of the temperature at which SSIE is carried out. Following exchange, the zeolite was characterized by infrared spectroscopy, temperature-programmed reduction with H_2, Cu and Cl K-edge XANES, and Cu K-edge EXAFS. By this means, information was obtained concerning the oxidation state and local environment of Cu cations within the zeolite. These studies revealed that the extent of reaction of Brønsted acid protons with CuCl is very sensitive to the temperature at which SSIE is carried out, as is the extent to which CuCl is occluded in the pores of the zeolite in the form of small $(CuCl)_n$ clusters.

Experimental Section

Catalyst Preparation. The ammonia form of ZSM-5 was obtained by exchanging NaZSM-5 (ALSI-PENTA SN-27, $SiO_2/Al_2O_3 = 23$, average crystal size 1−3 μm) with a 1 M NH_4NO_3 solution at 333 K twice. The resulting NH_4-ZSM-5 was calcined at 773 K for 3 h in air, and subsequently in He for 3 h. The as-prepared H-ZSM-5 was stored in a drybox and then mixed with CuCl (Cu/Al = 1 in moles). The mixture was finely ground using a mortar and pestle and transferred to a quartz reactor. Both operations were carried out in a drybox. The CuCl/H-ZSM-5 mixture was then exposed to He flowing at 50 cm^3/min, and the temperature was ramped at 2 K/min to 673, 823, 923, or 1023 K and kept at the desired temperature for 40 h. The resulting samples are denoted as Cu-ZSM-5(673), Cu-ZSM-5(823), Cu-ZSM-5(923), and Cu-ZSM-5(1023), respectively. All samples were stored in a drybox after preparation and until further use.

Catalyst Characterization. XRD data were collected with a Siemens D5000 diffractometer using Cu Kα radiation (45 kV and 35 mA) over a 2θ range of 5°−55° with step of 0.1° and residence time of 5 s at each point. Infrared spectra were recorded using a Nicolet Nexus 670 FTIR spectrometer equipped with an MCT-A detector. Measurements were taken using a resolution of 4 cm^{-1} and a total of 32 scans/spectrum. Samples were pressed into 30 mg of self-supporting pellets and subsequently placed into an infrared cell equipped with CaF_2 windows.

^{27}Al MAS NMR spectra were recorded at 130 MHz using a Bruker 500 spectrometer equipped with a 4 mm MAS probe. The ^{27}Al signals were referenced to an externally located aqueous solution of $Al(NO_3)_3$, which was used to calibrate the 90° flip for nonselective irradiation of all aluminum transitions. The ^{27}Al MAS NMR spectra of all zeolite samples were acquired using a 15° flip angle; 3200 scans were accumulated using a 1 s pulse delay. The MAS spinning speed was 12.0 kHz.

The gaseous products formed during SSIE of H-ZSM-5 with CuCl were analyzed by mass spectrometry. H_2O and HCl response factors were determined by reducing CuO and CuCl, respectively. For the study of SSIE of H-ZSM-5 by CuCl, 100 mg of a physical mixture of CuCl/H-ZSM-5 was placed in a quartz reactor and then

(27) Downing, S. R.; van Amstel, J.; Joustra, H. A. U.S. Patent, 4125483, 1978.
(28) Spoto, G.; Bordiga, S.; Ricchiardi, G.; Scarano, D.; Zecchina, A.; Geobaldo, F. *J. Chem. Soc.-Faraday Trans.* **1995**, *91*, 3285.
(29) Bolis, V.; Maggiorini, S.; Meda, L.; D'Acapito, F.; Turnes Palomino, G.; Bordiga, S.; Lamberti, C. *J. Chem. Phys.* **2000**, *113*, 9248.
(30) Spoto, G.; Bordiga, S.; Scarano, D.; Zecchina, A. *Catal. Lett.* **1992**, *13*, 39.
(31) Lamberti, C.; Bordiga, S.; Salvalaggio, M.; Spoto, G.; Zecchina A.; Geobaldo, F.; Vlaic, G.; Bellatreccia, M. *J. Phys. Chem. B* **1997**, *101*, 344.
(32) Prestipino, C.; Berlier, G.; Xamena, F. X. L. I.; Spoto, G.; Bordiga, S.; Zecchina, A.; Palomino, G. T.; Yamamoto, T.; Lamberti, C. *Chem. Phys. Lett.* **2002**, *363*, 389.
(33) Lamberti, C.; Bordiga, S.; Bonino, F.; Prestipino, C.; Berlier, G.; Capello, L.; D'Acapito, F.; Llabrés, I.; Xamena, F. X.; Zecchina, A. *Phys. Chem. Chem. Phys.* **2003**, *5*, 4502.
(34) Zecchina, A.; Bordiga, S.; Salvalaggio, M.; Spoto, G.; Scarano, D.; Lamberti, C. *J. Catal.* **1998**, *173*, 540.
(35) Zecchina, A.; Bordiga, S.; Palomino, G. T.; Scarano, D.; Lamberti, C.; Salvalaggio, M. *J. Phys. Chem. B* **1999**, *103*, 3833.
(36) Bolis, V.; Bordiga, S.; Palomino, G. T.; Zecchina, A.; Lamberti, C. *Thermochim. Acta* **2001**, *379*, 131.
(37) Turnes Palomino, G.; Zecchina, A.; Giamello, E.; Fisicaro, P.; Berlier, G.; Lamberti, C.; Bordiga, S. *Stud. Surf. Sci. Catal.* **2000**, *130*, 2915.
(38) Lamberti, C.; Palomino, G. T.; Bordiga, S.; Berlier, G.; D'Acapito, F.; Zecchina, A. *Angew. Chem.-Int. Ed.* **2000**, *39*, 2138.
(39) Bolis, V.; Bordiga, S.; Graneris, V.; Lamberti, C.; Turnes Palomino, G.; Zecchina, A. *Stud. Surf. Sci. Catal.* **2000**, *130*, 3261−3266.
(40) Spoto, G.; Zecchina, A.; Bordiga, S.; Ricchiardi, G.; Martra, G. *Appl. Catal. B.* **1994**, *3*, 151.
(41) Li, Zh.; Xie K.; Slade, C. T. R. *Appl. Catal. A* **2001**, *209*, 107.
(42) Drake, I. J.; Zhang, Y.; Gilles, M.; Liu T.; Nachimuthu, P.; Perera, R.; Bell, A. T. *J. Phys. Chem. B*, in press.
(43) Drake, I. J.; Zhang, Y.; Briggs, D.; Lim B.; Chau, T.; Bell, A. T. *J. Phys. Chem. B*, in press.

heated in a flow of He (50 cm^3/min) according to a prescribed temperature program.

Temperature-programmed reduction (TPR) of Cu-ZSM-5 with H_2 was carried out in a quartz microreactor. Prior to H_2-TPR, all catalysts (0.15 g) were contacted with He flowing at 50 cm^3/min and then heated to their preparation temperatures at 10 K/min. The samples were then cooled to room temperature in flowing He. The flow of He was then replaced by a 2% H_2/He mixture flowing at 30 cm^3/min. After the mass spectrometer response for H_2 had reached a constant value, the temperature was increased to 973 K at 10 K/min, and the responses for H_2, H_2O, and HCl were recorded simultaneously.

Cl K-edge XANES data were collected on Beamline 9.3.1 of the Advanced Light Source (ALS) at the Lawrence Berkeley National Laboratory. This beamline is equipped with a Si(111) double-crystal monochromator and a vacuum chamber that operates at 1.3×10^{-4} Pa. Spectra were recorded in fluorescence mode using a silicon photodiode detector (Hamamatsu model 3584-02). Energies were calibrated using Cs_2CuCl_4 as a reference. Scans were made between 2700 and 2923 eV with a 0.1 eV step in the edge region. Additional details concerning data acquisition and analysis can be found in ref 44.[44]

Cu K-edge X-ray absorption spectra were recorded in transmission mode using Beamline 2-3 at the Stanford Synchrotron Radiation Laboratory (SSRL). The station was operated with a double-crystal monochromator, containing a Si(111) crystal, detuned to 70% intensity to minimize the presence of higher harmonics. The samples were pressed into self-supporting wafers (calculated to have an absorbance of 2.5) and mounted in a controlled-atmosphere cell operated at 1 atm. EXAFS data were collected for each sample before and after heat treatment (at 673 K in He) at room temperature under He. The Cu K-edge of Cu foil, Cu_2O, CuO, and CuCl were also measured and used to obtain phase shifts and backscattering amplitudes for the Cu−Cu, Cu−O, and Cu−Cl absorber-backscatterer pairs.

Cu XANES data were analyzed with the IFEFFIT package. Pre-edge absorptions due to the background and detector were subtracted using a linear fit to the data in the range of 200 to 50 eV relative to the edge energy (E_0). Each spectrum was normalized by a constant determined by the average absorption in the range of 100−300 eV relative to E_0. The edge energy of each sample and reference was taken at the first inflection point beyond any pre-edge peaks.

Extraction of the EXAFS data from the measured absorption spectra was performed with the XDAP code.[45] The pre-edge was subtracted using a modified Victoreen curve. The background was subtracted by employing cubic spline routines with a continuously adjustable smooth parameter. Normalization was performed by dividing the data by the height of the absorption edge at 50 eV.

Data analysis was performed by multiple shell fitting in *R*-space using the EXAFS data-analysis program XDAP, which allows one to minimize the residuals between both the magnitude and the imaginary part of the Fourier transforms of the data and the fit. *R*-space fitting has significant advantages compared to the usually applied fitting in *k*-space and is discussed extensively in a recent paper by Koningsberger et al.[46] The difference file technique was applied together with phase-corrected Fourier transforms to resolve the different contributions in the EXAFS data. The difference file technique allows one to optimize each individual contribution with respect to the other contributions present in the EXAFS spectrum.[46] In this study, the EXAFS fits have been checked by applying *k* and k^3 weightings in order to be certain that the results are the same for all weightings.[47]

Table 1.

(a) Parameters Used in the Calculations for Generation of Theoretical References

atom pair	potential	σ^2 (Å^2)	S_0^2	V_r (eV)	V_i (eV)
Cu−O	Hedin-Linquist	0.003	0.84	9.0	4.0
Cu−Cl	Hedin-Linquist	0.004	0.84	4.0	5.6

(b) Best Fit Result for Experimental Cu_2O and CuCl Data Using Theoretical References[a]

atom pair	N	*R* (Å)	$\Delta\sigma$ (Å^2)	E_0 (eV)
Cu−O	2.0	1.85	0.004	−0.73
Cu−Cl	4.0	2.33	0.003	−0.11

[a] Fits were performed in *R*-space, k^3-weighted. Cu_2O: $\Delta k = 3-14$ Å^{-1}, $\Delta R = 1.0-1.8$ Å. CuCl: $\Delta k = 3-14$ Å^{-1}, $\Delta R = 1.0-2.5$ Å.

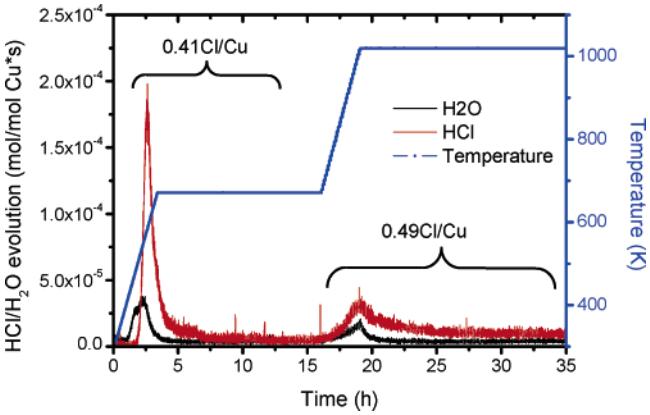

Figure 1. Evolution of HCl and H_2O during temperature-programmed heating of a mixture of CuCl and H-ZSM-5.

Theoretical phase shifts and backscattering amplitudes for the Cu−O and Cu−Cl absorber-scatterer pairs were used in EXAFS data analysis, which were generated utilizing the FEFF8 code with the parameters listed in Table 1a. The theoretical references were calibrated using experimental data for Cu_2O and CuCl, employing the procedure reported in ref 46. Table 1b gives the best fit result for the experimental data using the theoretical references. The fitted EXAFS coordination parameters correspond with the crystallographic values for Cu_2O ($N = 2$ and $R = 1.85$ Å and CuCl ($N = 4$ and $R = 2.33$ Å).

Results and Discussion

Figure 1 shows the evolution of HCl and H_2O during the temperature-programmed heating of a physical mixture of CuCl and H-ZSM-5. When the temperature is raised from 298 to 673 K at 2 K/min, HCl is evolved in the integral amount of 0.41 HCl/Cu. The evolution of H_2O begins just ahead of the evolution of HCl and declines to zero as the HCl peak reaches its maximum. No further HCl or H_2O is released while the temperature is maintained at 673 K for up to 10 h. However, a further increase in the temperature from 673 to 1023 K results in the simultaneous release of additional HCl and H_2O. In this case, the evolution of HCl

(44) Drake, I. J.; Fujdala, K. L.; Bell, A. T.; Tilley, T. D. *J. Catal.* **2005**, *230*, 14.
(45) Vaarkamp, M.; Linders, J. C.; Koningsberger, D. C. *Physica B* **1995**, *208/ 209*, 159.
(46) Koningsberger, D. C.; Mojet, B. L.; van Dorssen, G. E.; Ramaker, D. E. *Top. Catal.* **2000**, *10*, 143.
(47) Ros, T. G.; Keller, D. E.; van Dillen, A. J.; Geus, J. W.; Koningsberger, D. C. *J. Catal.* **2002**, *211*, 85.

Table 2. Effects of Temperature of SSIE on the Cu, Al, and Cl Content of Cu-ZSM-5 Determined by Elemental Analysis[a]

catalyst	Cu (wt %)	Al (wt %)	Cl (wt %)	Cu/Al	Cl/Cu
Cu-ZSM-5(673)	6.6	3.3	0.7	0.85	0.21
Cu-ZSM-5(823)	7.4	3.3	0.6	0.96	0.15
Cu-ZSM-5(923)	7.1	3.3	0.3	0.90	0.08
Cu-ZSM-5(1023)	6.8	3.2	0.5	0.87	0.16

[a] All elemental analyses are accurate to ±10%.

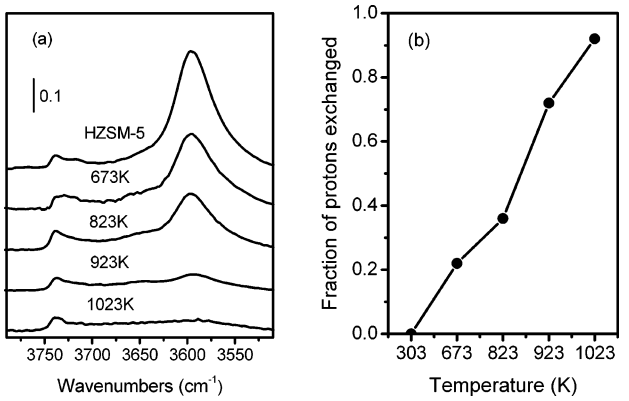

Figure 2. Infrared spectra of Cu-ZSM-5 prepared at different temperatures (a) and the extent of proton exchange by Cu^+ based on the area of the band at 3610 cm^{-1} (b).

declines slowly during the 15 h that the sample is held at 1023 K. The integral amount of HCl released in the second peak is 0.49 HCl/Cu. Thus, an aggregate of 0.90 HCl/Cu is evolved over the full course of SSIE. It is tempting to associate the evolution of HCl solely with the reaction of CuCl with Brønsted acid protons (ZH + CuCl → ZCu + HCl); however, CuCl can also react with residual H_2O in the zeolite to form Cu_2O ($2CuCl + H_2O \rightarrow Cu_2O + 2HCl$) or CuOH ($CuCl + H_2O \rightarrow CuOH + HCl$). Consequently, additional sample characterization must be carried out in order to establish the extent to which each of these processes contributes to the evolution of HCl.

Elemental analyses of the Al, Cu, and Cl contents of samples of Cu-ZSM-5 prepared by SSIE at 673, 823, 923, and 1023 K are listed in Table 2. It is evident that the Al and Cu contents of the samples expressed as fractions of the weight of the zeolite alone do not depend strongly on the temperature at which ion exchange is carried out, and that the atomic Cu/Al ratio lies in the range of 0.85−0.96, which is close to that used in the CuCl/H-ZSM-5 mixture prior to SSIE, 1.0, suggesting that little, if any, CuCl is lost during the course of exchange. This conclusion is consistent with visual observation, which showed no evidence for the deposition of CuCl on the walls of the quartz tube downstream of the heated portion of the tube. What is notable is that the Cl content measure after ion exchange decreases with increasing exchange temperature, but then rises for the sample prepared at 1023 K.

Figure 2a illustrates the infrared spectrum for the O−H stretching region. Spectra are shown for the original H-ZSM-5 and for samples of Cu-ZSM-5 prepared at temperatures of 673−1023 K. With increasing exchange temperature, the intensity of the band at 3610 cm^{-1}, which is characteristic of Brønsted acid protons,[48] decreases monotonically and approaches zero at 1023 K. The extent of proton exchange by Cu^+ is shown in Figure 2b. Figure 2a also shows that the infrared peak at 3740 cm^{-1}, which is characteristic of Si−OH groups,[48] is essentially unaltered during the course of cation exchange with CuCl.

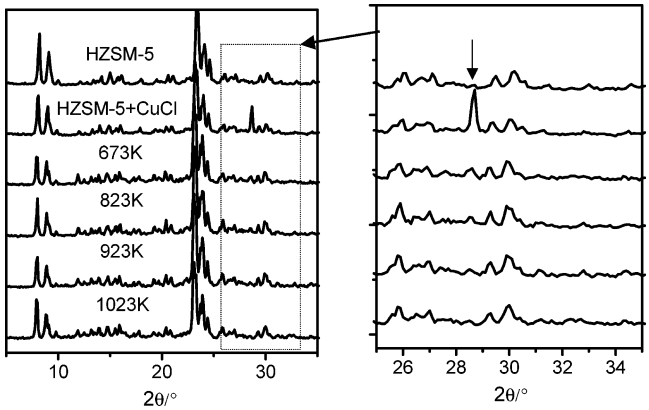

Figure 3. Effect of SSIE temperature on the XRD pattern of Cu-ZSM-5. XRD patterns for H-ZSM-5 and for a physical mixture of CuCl and H-ZSM-5 are shown for comparison. The inset shows a single peak from the diffraction pattern of CuCl.

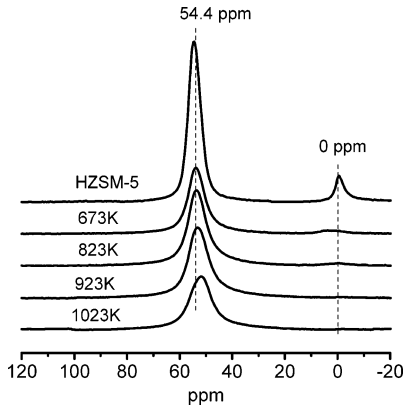

Figure 4. Effect of SSIE temperature on the ^{27}Al MAS NMR spectrum of Cu-ZSM-5.

XRD patterns for H-ZSM-5, for a mixture of HZSM-5 and CuCl, and Cu-ZSM-5 prepared at different exchange temperatures are shown in Figure 3. It is evident that the MFI structure of the zeolite is retained as the temperature at which SSIE is carried out increases. A peak at 28.6° can be seen in the diffraction pattern of the mixture of H-ZSM-5 and CuCl, which is characteristic of crystalline CuCl. As the temperature of exchange increases, the intensity of this peak decreases rapidly and is no longer visible in the XRD pattern of the sample of Cu-ZSM-5 prepared at 1023 K.

^{27}Al NMR spectra of H-ZSM-5 and Cu-ZSM-5 prepared at temperatures between 673 and 1023 K are shown in Figure 4. In all cases, spectra were taken after sample equilibration with ambient water vapor in order to relax the lattice strain and create a more symmetric environment around the Al nucleus. By doing so, the effect of the ^{27}Al quadropole moment on the width of the NMR peaks is diminished. Peaks at 54 and 0 ppm are seen in the spectrum of H-ZSM-5, corresponding to tetrahedrally and octahedrally coordinated Al, respectively.[42,49] The peak for octahedrally coordinated

(48) Zecchina, A.; Bordiga, S.; Spoto, G.; Scarano, D.; Petrini, G.; Leofanti, G.; Padovan, M.; Otero A. C. *J. Chem. Soc., Faraday Trans.* **1992**, *88*, 2959.

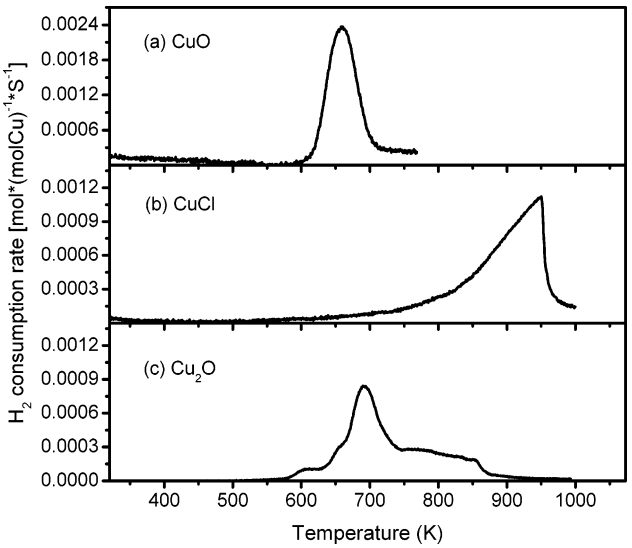

Figure 5. H_2-TPR spectra of CuO (a), CuCl (b), and Cu_2O (c).

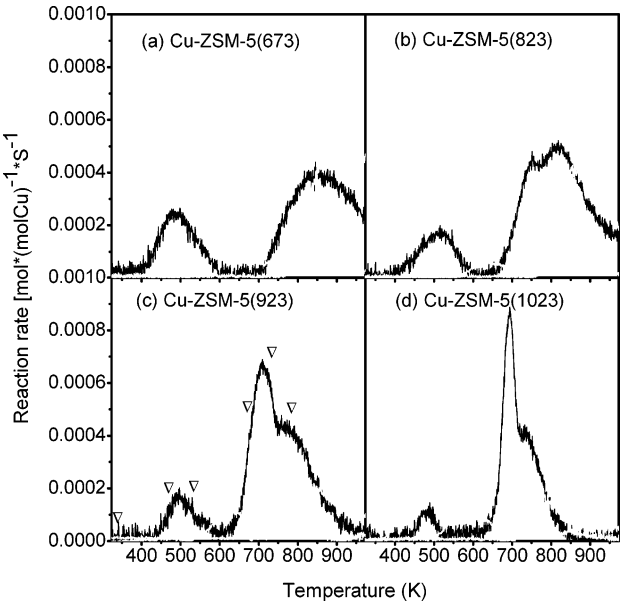

Figure 6. Effect of SSIE temperature on the H_2-TPR of Cu-ZSM-5. (a) Cu-ZSM-5(673); (b) Cu-ZSM-5(823); (c) Cu-ZSM-5(923); (d) Cu-ZSM-5(1023). [H_2 consumption (dark line), H_2O production (gray line), and HCl production (light gray line)].

Al is due to the strong interaction of H_2O with Brønsted acid protons.[42,49] When the Brønsted acid protons are exchanged with Cu^+ cations, this peak disappears and the peak for tetrahedrally coordinated Al broadens, and the integrated peak intensity decreases. These effects are a consequence of paramagnetic Cu^{2+} cations present in the zeolite. A similar effect has been reported for Fe-ZSM-5 and is attributed to a shortening of the nuclear relaxation time of the framework Al atoms by the presence of paramagnetic species.[50] A small upfield shift in the position of the peak for the tetrahedrally coordinated line is also observed, which is attributable to a change in the shielding of the Al nucleus caused by the Cu^+ cations.

Temperature-programmed reduction (TPR) of Cu-ZSM-5 was carried out in order to obtain additional information about the form in which Cu is present in the zeolite after SSIE at different temperatures. For reference, TPR spectra were obtained as well, for pure Cu_2O, CuCl, and CuO. The TPR spectra of the standards are shown in Figure 5. The maximum rate of H_2 consumption during the reduction of CuO occurs at ~658 K, whereas the reduction of CuCl starts at 773 K and reaches a maximum rate at ~951 K. Cu_2O exhibits a peak in the rate of H_2 consumption at ~693 K, together with a shoulder at 613 K and a tail in the range from 742 to 863 K.

The H_2 consumption rate and the rates of H_2O and HCl evolution observed during TPR of Cu-ZSM-5 prepared at different temperatures are shown in Figure 6. Two principal features are observed in the plots of H_2 consumption as a function of temperature. The first feature is a peak at 475 K, which is followed by the release of water at about 600 K, but not HCl. As the temperature at which SSIE is carried out increases, the first peak for hydrogen consumption decreases in intensity. The position of this peak is similar to that reported previously for the TPR of Cu-ZSM-5 that had been oxidized prior to the start of reduction.[22−25] Analysis of XANES and EXAFS data taken as a part of these studies indicate that prior to reduction all of the copper is present as Cu^{2+} and that the reduction peak observed in the temperature range of 400−500 K is attributable to the reduction of Cu^{2+} to Cu^+ and Cu^+ to Cu^0. The position of the first reduction peak observed in Figure 6 is substantially lower than that observed for bulk CuO or Cu_2O, suggesting that it is not likely due to the reduction of these compounds. The alternative is that some of the copper following SSIE is present as exchanged Cu^{2+} cations, charge-compensated by two next-nearest neighbor charge-exchange sites in the zeolite, or as $[CuOCu]^{2+}$ or $[Cu(OH)_2Cu]^{2+}$ dimer cations (i.e., Z[CuOCu]Z or Z[Cu(OH)$_2$Cu]Z). However, as discussed below, no evidence was found for Cu^{2+} in the XANES spectra taken of the catalyst. While this does not exclude the possibility for the presence of such cations, it suggests that their concentration if present is low (<10%). Furthermore, failure to see the reappearance of an infrared band for Brønsted acid protons upon reduction in the temperature range of the first TPR peak (see below) suggests that the Cu species undergoing reduction are occluded in the zeolite lattice, rather than being charge-compensated by the lattice. Candidate structures for such species could be nanoclusters of Cu_2O or CuOH formed via the reaction of water vapor with CuCl during the course of SSIE. For reasons discussed below, we believe that it is more likely that the occluded material is Cu_2O.

The second feature seen in the TPR spectra of Figure 6 occurs near 850 K when SSIE is carried out at 673 K. This feature evolves into two features as the temperature of SSIE increases: the first centered at about 700 K and the second centered at about 750−800 K. The second of these two peaks is very likely due to the reduction of occluded CuCl since it is accompanied by an intense peak for the release of HCl. Some H_2O is also released in association with the higher temperature component, possibly due to the condensation

(49) Joyner, R. W.; Smith, A. D.; Stockenhuber, M.; van den Berg, M. W. E. *Phys. Chem. Chem. Phys.* **2004**, *6*, 5435.
(50) Marturano, P.; Drozdová, L.; Kogelbauer, A.; Prins, R. *J. Catal.* **2000**, *192*, 236.

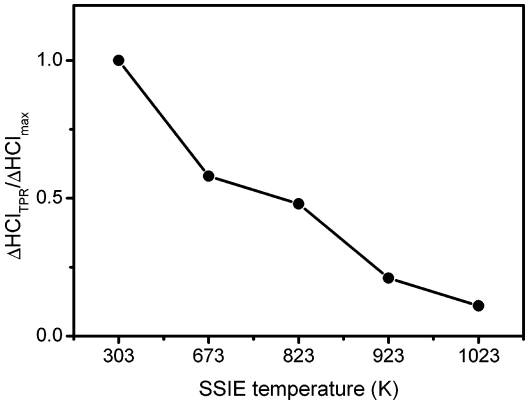

Figure 7. Effect of SSIE temperature on HCl evolution during H_2-TPR of Cu-ZSM-5.

Table 3. Effects of Temperature of SSIE on the Fractions of Cu in Cu-ZSM-5 Present as Exchanged Cu^+ Cations (ZCu), CuCl, and Cu_2O Prepared with Different Treatment Temperatures

catalyst	ZCu/Al	CuCl/Al	$2Cu_2O$/Al
Cu-ZSM-5(673)	0.22	0.58	0.20
Cu-ZSM-5(823)	0.36	0.48	0.16
Cu-ZSM-5(923)	0.72	0.20	0.08
Cu-ZSM-5(1023)	0.92	0.10	0.00[a]

[a] NB failure of the fractions to sum to 1.0 is a reflection of the experimental accuracy.

of Si−OH groups. With increasing temperature of SSIE, the intensities of the reduction peaks attributed to Cu_2O and CuCl decrease and a new H_2 consumption peak appears at 750 K. This latter peak becomes the dominant feature in the TPR spectrum and shifts to 650 K when SSIE is carried out at 1023 K. This feature is attributed to the reduction of Cu^+ cations that have been exchanged for Brønsted acid protons (i.e., ZCu). The reduction of these species is not accompanied by the release of either H_2O or HCl, but does result in the reappearance of Brønsted acid protons (i.e., $ZCu + {}^1/_2H_2 \rightarrow ZH + Cu^0$), a process that is observed via infrared spectroscopy (see below).

Taken together, the results of the TPR experiments suggest that when SSIE is carried out at 673 K much of the CuCl is occluded into the pores of the zeolite as X-ray amorphous clusters of CuCl, and to a lesser extent as clusters of Cu_2O. As the temperature at which SSIE is carried out increases, Figure 7 shows that the total amount of HCl released relative to the maximum that could be released if all of CuCl used for exchange were reduced to Cu and HCl decreases monotonically. Using these results and those in Figure 2b, it is possible to estimate the distribution of Cu present after SSIE at a given temperature. Table 3 shows that as the exchange temperature rises from 673 to 1023 K, the fraction of the initial Cu that is exchanged for protons rises from 0.22 to 0.90, whereas the fraction of the initial Cu that is occluded as CuCl decreases from 0.58 to 0.10, and the fraction of the initial Cu that is occluded as Cu_2O decreases from 0.20 to 0.16 at 823 K, and then further decreases to 0.0 at higher temperatures. This interpretation is supported by the infrared spectra shown in Figure 8, which were taken in situ during the TPR of the sample of Cu-ZSM-5 prepared at 923 K. At room temperature, the intensity of the peak at 3610 cm^{-1} for Brønsted acid protons is ∼0.25 of its maximum intensity if all of the cation-exchange sites are

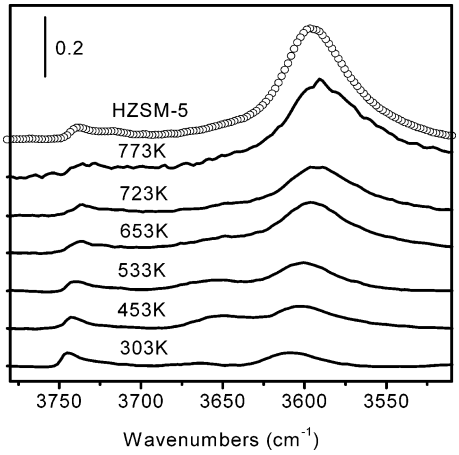

Figure 8. Infrared spectrum of Cu-ZSM-5(923) acquired during H_2-TPR and H-ZSM-5.

occupied by protons. As the reduction temperature rises, the intensity of this band remains essentially constant between 303 and 533 K, the temperature interval over which Cu_2O undergoes reduction (see Figure 6). For reduction temperatures above 533 K, the intensity of the band for Brønsted acid protons increases and reaches its maximum at 773 K. Figure 6 shows that the temperature interval from 600 to 773 K corresponds to a regime in which ZCu undergoes reduction via the process $ZCu + {}^1/_2H_2 \rightarrow ZH + Cu^0$. The fraction of Cu undergoing this process is 0.75 of the total Cu used for the exchange process, in excellent agreement with the results shown in Table 3.

The distribution of species reported in Table 3 is also consistent with the data presented in Figure 1. For exchange carried out at 673 K, Figure 1 shows that 0.41 mol of HCl are released per mole of Cu present originally as CuCl. Table 3 indicates that 0.22 mol of HCl/mol of CuCl used for SSIE are released via the reaction $ZH + CuCl \rightarrow ZCu + HCl$. If it is assumed that the Cu_2O listed in Table 3 is formed via the reaction $2CuCl + H_2O \rightarrow Cu_2O + 2HCl$, then one can calculate that the total amount of HCl that should have been released during SSIE at 673 K due to this process would be 0.20 mol/mol of CuCl used for SSIE. By this means we can estimate that 0.42 mol of HCl should have been released during SSIE at 673 K/mol of CuCl used for the exchange process. This figure agrees closely with the value of 0.41 mol of HCl/mol of CuCl shown in Figure 1. Likewise, for SSIE carried out at 1023 K, Table 3 indicates that 0.90 mol of HCl should have been released per mole of CuCl via the process $ZH + CuCl \rightarrow ZCu + HCl$, and that there should be no other sources of HCl, since little Cu_2O is formed in this case. The anticipated figure for the release of HCl is in perfect agreement with what is observed in Figure 1. This analysis further supports the attribution of the low-temperature hydrogen consumption peak observed in Figure 6 to the reduction of clusters of Cu_2O formed via hydrolysis of occluded CuCl.

X-ray absorption near-edge spectroscopy (XANES) was used to obtain additional information about the oxidation state and coordination of Cu in Cu-exchanged ZSM-5. XANES spectra were obtained for Cu_2O, CuCl, Cu foil, and CuO. Panels (a) and (b) in Figure 9 show the XANES spectra and the corresponding derivative curves for these reference

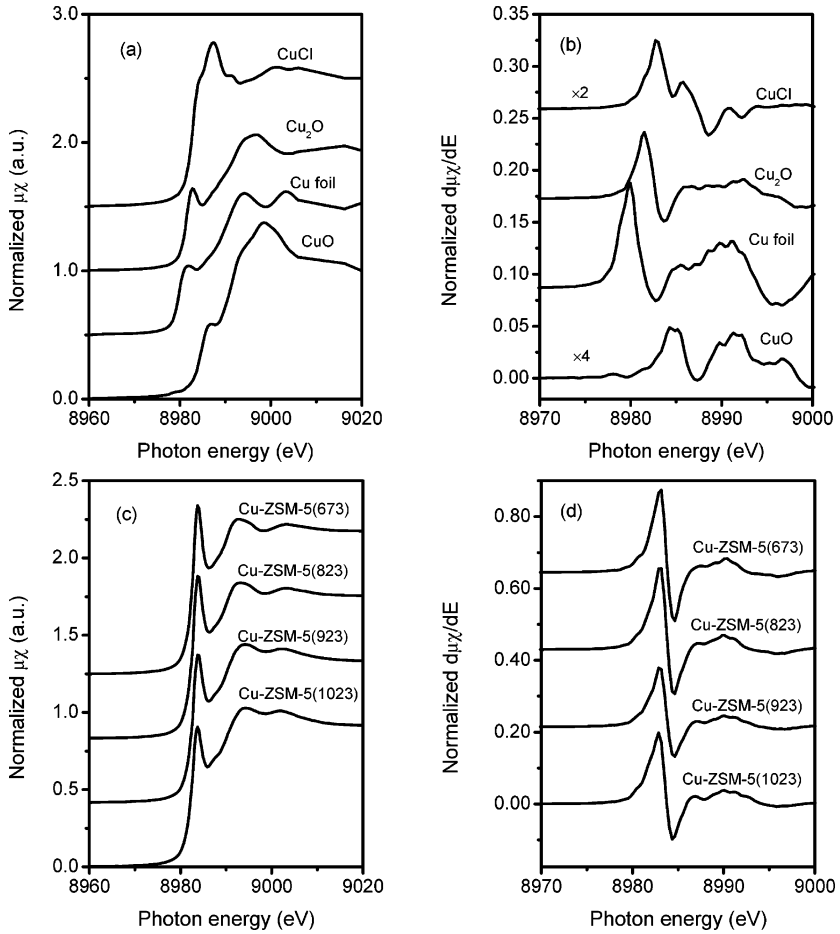

Figure 9. Cu K-edge XANES features of standards (a) and Cu-ZSM-5 (c) and the corresponding derivative curves (b) and (d), respectively.

Table 4. Cu K-edge XANES Features of Standards and Cu-ZSM-5 Catalysts

standard	E_0[a] (eV)	pre-edge feature (eV)[b]	1s→3d[c] (eV)
CuCl	8982.8	8984.6	
Cu_2O	8981.5	8982.8	
Cu foil	8980.0	8981.7	
CuO	8984.3	8986.7	8978.3
Cu-ZSM-5	~8983.0	8983.9	

[a] Edge energy determined by the first inflection point. [b] Position of peak or shoulder on the rising edge (1s→4p). [c] Position of peak.

compounds. The corresponding edge energies and energies for specific electronic transitions are listed in Table 4. For Cu metal (Cu^0), the inflection point is at 8980 eV and the pre-edge peak due to the dipole-allowed 1s−4p electronic transition is at 8981.7 eV.[29,51] Cu_2O exhibits a well-defined pre-edge peak at 8982.8 eV and a peak maximum at 8996.7 eV. The pre-edge peak lies in an energy range (8982−8985 eV) that is characteristic of 1s−$4p_{xy}$ transitions of Cu(I) in low coordination environments.[52] CuCl shows a shoulder at 8984.6 eV and a very intense peak at 8987.3 eV. CuO exhibits three features in the XANES region: a weak absorption at about 8975−8979 eV, attributed to the dipole-forbidden 1s−3d electronic transition; a 1s−4p transition, which produces a shoulder at 8986.7 eV; and a very intense peak at 8998 eV, all of which are characteristic of Cu^{2+}.[32]

Panels (c) and (d) in Figure 9 show Cu K-edge XANES spectra and the corresponding derivative curves for Cu-ZSM-5 prepared by SSIE at different temperatures. A single, well-defined peak at 8983.8 eV is observed for all samples characteristic of the dipole-allowed 1s−4p electronic transition of Cu^+. The absence of Cu^{2+} and Cu^0 features rules out the presence of CuO or Cu metal species in copper-exchanged samples. The absence of a peak at 8987.3 eV in the XANES region also suggests the absence of any bulk CuCl, consistent with what is seen in the XRD patterns shown in Figure 3. Surprisingly, the samples prepared at 673 and 823 K both exhibit a very sharp peak at 8983.8 eV, similar to that seen for the samples prepared at 923 and 1023 K, but more intense. This feature has been assigned to the 1s−$4p_{x,y}$ electron transition of Cu^+ species in a linear or planar configuration, which are doubly or triply coordinated, respectively.[31,33] Reduction in symmetry is believed to cause a decrease in the intensity of the 1s−4p electron transition, due to the increased Laporte-forbidden character of the p orbital. XANES studies of 19 Cu(I) compounds by Kau et al.[40] have shown that the transition from the 1s state to the doubly degenerate $4p_{x,y}$ state results in an intense pre-edge peak for two-coordinated complexes with the exception of Cu_2O. Triply coordinated Cu(I) complexes generally exhibit a less intense pre-edge peak when the copper has a T-shaped or trigonal planar geometry. Thus, the intensity of the 1s−4p transition decreases with increasing coordination number of copper, and hence, the sharper and more intense 1s−$4p_{x,y}$

(51) Drake, I. J.; Fujdala, K. L.; Baxamusa, S.; Bell, A. T.; Tilley, T. D. *J. Phys. Chem. B* **2004**, *108*, 18421.
(52) Kau, L.-Sh.; Spira-Solomon, D. J.; Penner-Hahn, J. E.; Hodgson, K. O.; Solomon, E. I. *J. Am. Chem. Soc.* **1987**, *109*, 6433.

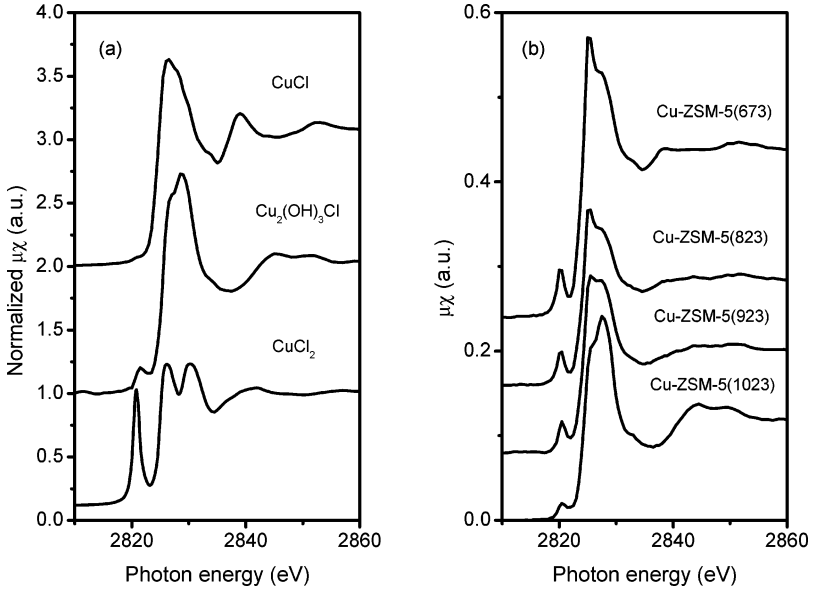

Figure 10. Cl K-edge XANES of standards (a) and Cu-ZSM-5 (b).

electron transition for Cu-ZSM-5 prepared at 673 and 823 K is attributed to a lower degree of Cu coordination. Fulton et al.[53] have reported XANES spectra for a linear dichloro Cu(I) species, $CuCl_2^-$, which shows a very similar pre-edge peak to that seen in Cu-ZSM-5(673). It has been found [31] that copper-exchanged ZSM-5 has triply coordinated and doubly coordinated Cu^+ cations in equal proportion. Therefore, with increasing degree of exchange, the observed decrease in the intensity of pre-edge peak of Cu-ZSM-5(923) and Cu-ZSM-(1023) reflects an increase in the amount of triply coordinated Cu.

Cl K-edge XANES spectra were acquired in order to identify the nature of the Cl remaining in the zeolite after SSIE. Figure 10a shows reference spectra for CuCl, $Cu_2(OH)_3Cl$ (paratacamite), and $CuCl_2$, and Figure 10b shows similar spectra for Cu-ZSM-5 prepared at different exchange temperatures. The XANES data in Figure 10b confirm that Cl is retained in the zeolite, independent of the exchange temperature. Comparison of the peaks in Figures 10a and 10b suggests that the principle Cl-containing species in Cu-ZSM-5(673) and Cu-ZSM-5(823) is CuCl, whereas that in Cu-ZSM-5(1023) is a mixture of CuCl and $Cu_2(OH)_3Cl$. The latter compound can be envisioned to form via the reaction $2CuCl + 2H_2O + {}^1/_2O_2 \rightarrow Cu_2(OH)_3Cl + HCl$ during air exposure of the freshly prepared Cu-ZSM-5. It is noted further that all of the Cl K-edge XANES spectra contain a well-defined peak at ~2820 eV that is characteristic of Cl associated with Cu^{2+} cations. Figure 10a shows that this peak is much weaker in the spectrum of $Cu_2(OH)_3Cl$ than $CuCl_2$, which suggests that some $CuCl_2$ may be present in all of the samples after prior air exposure. The formation of $Cu(OH)_3Cl$ and $CuCl_2$ can be envisioned to occur via the following process: $2CuCl + 2H_2O + {}^1/_2O_2 \rightarrow Cu_2(OH)_3Cl + HCl$ and $2CuCl + {}^1/_2O_2 + 2HCl \rightarrow 2CuCl_2 + H_2O$. It is quite likely that since CuCl is highly dispersed as small clusters (see below) it is reactive in ambient air at room temperature. The formation of Cu^{2+} cations via either process could be the reason the ^{27}Al NMR peaks for Cu-ZSM-5 seen in Figure 4 are paramagnetically broadened.

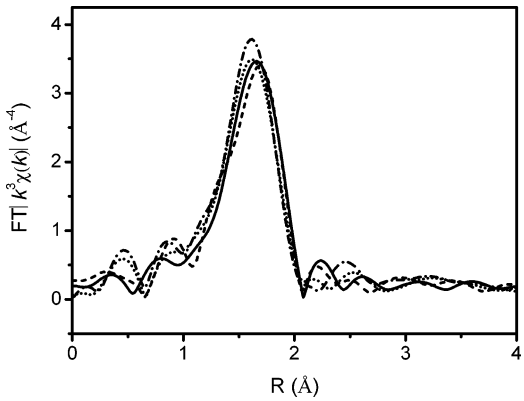

Figure 11. Fourier transforms of experimental data on Cu-ZSM-5 prepared at different temperatures (k^3 weighted, $\Delta k = 3-13$ Å^{-1}, phase-uncorrected), Cu-ZSM-5(673) (solid line), Cu-ZSM-5(823) (dotted line), Cu-ZSM-5(923) (dashed line), and Cu-ZSM-5(1023) (dot−dashed line).

The local environment of Cu cations in ZSM-5 was further characterized using Cu K-edge EXAFS. The Fourier transforms of the k^3-weighted scattering function, $\chi(k)$, for Cu-ZSM-5 prepared at different temperatures are shown in Figure 11. The main contributions are in the range of 1.0−2.0 Å. With increasing exchange temperature, the peak shifts to lower values of R accompanied by a slight increase in intensity. Changes also occurred in the region of high R, and a new contribution arises around 2.5 Å when the exchange temperature is higher than 923 K. This new feature is attributable to Cu−Al backscattering.[42] To identify the types of scattering atoms in proximity to Cu absorbers, the phase-correction technique was applied to the experimental data. Phase-corrected Fourier transformation should lead to a single peak with a symmetrical imaginary part, having its maximum at the maximum of the absolute magnitude and at the right coordination distance. If this correspondence is not observed, then extra sources of backscattering must be considered. Phase-corrected FT spectra (referenced to Cu−O) are shown in Figure 12. For Cu-ZSM-5(1023), phase correction leads to an optical spectrum, exhibiting a maxi-

(53) Fulton, J. L.; Hoffmann, M. M.; Darab, J. G. *Chem. Phys. Lett.* **2000**, *330*, 300.

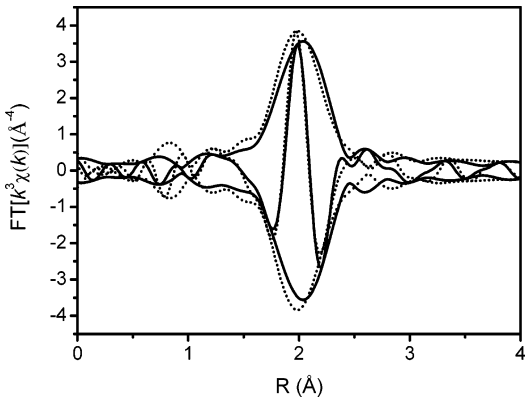

Figure 12. Fourier transforms of experimental data for Cu-ZSM-5(673) (solid line) and Cu-ZSM-5(1023) (dotted line) (k^3 weighted, $\Delta k = 3-13$ Å^{-1}, Cu−O phase-corrected).

mum in the imaginary component, which coincides in position with the maximum in the absolute magnitude. The agreement in the positions of the peaks in the magnitude and imaginary component confirms that backscattering in Cu-ZSM-5(1023) is predominantly from O atoms. However, for Cu-ZSM-5(673) and Cu-ZSM-5(823) the maximum of the imaginary part lies to the left of the maximum of the magnitude. This relationship is strongly indicative of more than one type of backscatterer. Phase correction using the Cu−Cl reference (CuCl) was also tested, but this too did not lead to a symmetric peak in the magnitude. Thus, there is little doubt that the first peak in the FT of $k^3\chi(k)$ for Cu-ZSM-5(673) and Cu-ZSM-5(823) contains contributions due to Cu−O and Cu−Cl backscattering. It is also possible that a small portion of the backscattering seen in the FT spectra of Cu-ZSM-5(923) and Cu-ZSM-5(1023) is due to the residual Cl atoms present around some of the copper absorbers.

Analysis of the EXAFS data for copper-exchanged zeolites catalysts was performed by multiple-shell fitting in *R* space over the range of $1 < R < 2$ Å. Cl backscattering was included for all samples. The difference file technique was applied together with phase-corrected Fourier transformation to resolve the different contributions to the EXAFS data. The difference file technique allows one to optimize each individual contribution with respect to the other contributions present in the EXAFS spectrum. The EXAFS coordination parameters are given in Table 5. For Cu-ZSM-5(673), the Cu−Cl first shell coordination number is 1.3 and the Cu−Cl distance is 2.16 ± 0.02 Å, whereas the Cu−O coordination number is 1.2 and the Cu−O distance is 1.95 ± 0.02 Å. With increasing exchange temperature, the number of neighboring Cl atoms decreases, and the number of

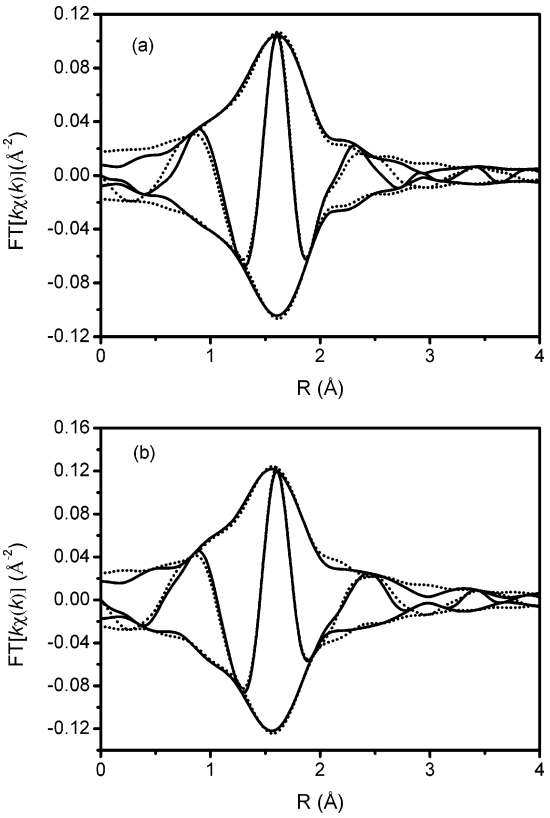

Figure 13. Fourier transforms (k^1 weighted, $\Delta k = 3.0-13.0$ Å^{-1}) of the experimental data (solid line) and total fit (dotted line) for Cu-ZSM-5(673) (a) and Cu-ZSM-5(1023) (b).

oxygen neighbors increases from 1.2 to 2.5, while the Cu−O distance increases from 1.95 to 1.97 Å. For Cu-ZSM-5(1023), each copper atom has 0.2 Cl neighbors at 2.22 ± 0.02 Å and 2.5 O neighbors at 1.97 ± 0.02 Å.

Figure 13 compares the Fourier transforms of the experimental EXAFS and the best fit of Cu-ZSM-5(673) and Cu-ZSM-5(1023). Similar results were obtained for Cu-ZSM-5(823) and Cu-ZSM-5(923) but are not shown. Good agreement between the fitted transforms and the ones based on experimental data demonstrates that backscattering elements (O and Cl) have been properly chosen. An illustration of the contributions to Cu backscattering from Cu−O and Cu−Cl is presented in Figure 14a for Cu-ZSM-5(673). This figure shows the Fourier transform of the difference file for the Cu−O contributions (raw data minus calculated Cu−Cl contribution) and for the fitted FT of Cu−O backscattering. It is evident that the fitted spectra are in a good agreement with the Cu−O difference file spectrum both for the magnitude and the imaginary part. The peak in the magnitude is located at about 1.95 Å. The agreement between the fitted

Table 5. Fit Parameters of EXAFS Spectra (Δk: 3−13 Å^{-1}, ΔR: 1.0−2.0 Å) and Variances for Model Spectra of Cu-ZSM-5 Catalysts

catalyst	scatterer	*N* (±10%)	*R* (Å, ±0.02 Å)	$\Delta\sigma^2$ (10^{-3} Å^2, ±5%)	ΔE_0 (eV, ±10%)	*k*-variance (%) Im.	Abs.
Cu-ZSM-5(673)	Cl	1.3	2.16	1.3	1.0	0.62	0.09
	O	1.2	1.95	1.5	−1.4		
Cu-ZSM-5(823)	Cl	1.1	2.17	1.0	−0.6	0.49	0.10
	O	1.5	1.96	3.8	−0.2		
Cu-ZSM-5(923)	Cl	0.5	2.18	3.0	−3.9	0.41	0.09
	O	2.3	1.97	3.6	−1.3		
Cu-ZSM-5(1023)	Cl	0.2	2.22	2.1	−6.8	0.35	0.10
	O	2.5	1.97	3.1	−1.7		

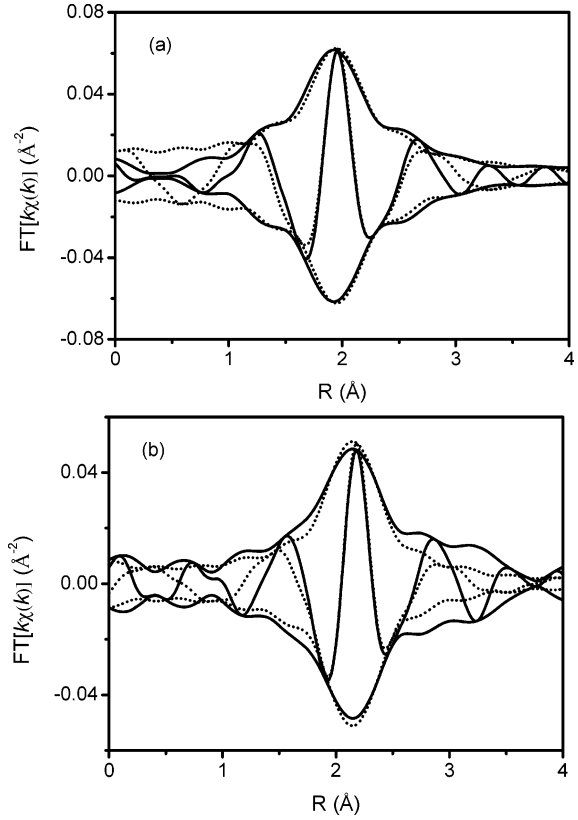

Figure 14. (a) Fourier transforms (k^1 weighted, $\Delta k = 3-11$ Å^{-1}, Cu−O phase-corrected) of the Cu−O difference file (raw spectra minus fitted Cu−Cl contribution, solid line) and fitted Cu−O contributions (dotted line) and (b) Fourier transforms (k^1 weighted, $\Delta k = 3-11$ Å^{-1}, Cu−Cl phase-corrected) of the Cu−Cl difference file (raw spectra minus fitted Cu−O contribution, solid line) and fitted Cu−Cl contributions (dotted line) of Cu-ZSM-5(673).

spectrum and the Cu−Cl difference file spectrum is shown in Figure 14b. The position of the peak in the magnitude occurs at 2.15 Å.

The preceding discussion, together with the H_2 TPR data presented in Figure 6, demonstrates that CuCl is retained in the pores and intersections of ZSM-5. An important question, though, is the form of this occluded CuCl. In crystalline CuCl each copper atom has 4 Cl neighbors located at a distance of 2.34 Å. Since the Cu−Cl coordination numbers are significantly smaller than 4 and the corresponding bond distances are shorter than 2.34 Å in all of the samples of Cu-ZSM-5, the presence of bulk CuCl can be ruled out. The XRD patterns presented in Figure 3 also support this conclusion. Thus, CuCl must be present in another form. Hargittai et al.[54] have reported that, at 689 K, CuCl vapor consists mainly of Cu_3Cl_3 and Cu_4Cl_4 clusters, whereas Cu_2Cl_2 clusters are found in high concentration at 1333 K. All the clusters are comprised of planar rings and each copper has two chlorine neighbors in its nearest shell. At 689 K, the Cu−Cl bond lengths are 2.166 ± 0.008 Å and 2.141 ± 0.008 Å for the trimer and tetramer, respectively. A distance of 2.254 ± 0.011 Å was determined for CuCl dimers at 1333 K, and the bond distances for the trimer and tetramer increased to 2.180 and 2.155 Å, respectively. The Cu−Cl bond lengths and coordination numbers for CuCl oligomers are similar to those determined for Cu-ZSM-5. This suggests that CuCl trimers and/or tetramers are the predominant species present in Cu-ZSM-5(673) and Cu-ZSM-5(823), which are characterized by Cu−Cl distances of 2.16 and 2.17 Å, respectively. Such clusters have D_{3h} and D_{4h} symmetry, which would explain the very intense $1s-4p_{x,y}$ electron transition observed in the XANES spectra of Cu-ZSM-5(673) and Cu-ZSM-5(823). When the exchange temperature is increased to 1023 K, the Cu−Cl bond distance increases to 2.22 Å, which is more characteristic of CuCl dimers. Consistent with this interpretation, we note that 10% of the Cu present in Cu-ZSM-5(1023) is present as CuCl (see Table 2) and the average Cu−Cl coordination number is 0.2 (see Table 5), which means that the coordination number for the Cu atoms bound to Cl is in reality 2, in excellent agreement with the proposal that the occluded CuCl in Cu-ZSM-5(1023) is present largely as Cu_2Cl_2.

Based on the above calculations, the actual Cu−O coordination number for Cu-ZSM-5(1023) number is ∼2.7, which suggests that the Cu^+ cations are both triply and doubly coordinated. This conclusion agrees with earlier work by Zecchina and co-workers, which reported an apparent Cu−O coordination number of 2.5.[31] Examination of the MFI structure shows that, in fact, cation-exchange sites exist that involve two and three lattice oxygen atoms. Therefore a Cu coordination number of 2.7 means that 70% of the Cu^+ cations are triply coordinated and 30% are doubly coordinated to O atoms. The Cu−O distance of 1.98 ± 0.02 Å reported here is also consistent with that reported earlier.[31]

Conclusions

The solid-state ion exchange of H-ZSM-5 and CuCl involves the following steps: (i) CuCl vaporization to form trimers and tetramers at a temperature higher than 673 K; (ii) diffusion of copper chloride oligomers into the pores and intersections of H-ZSM-5; (iii) dissociation of CuCl oligomers and reaction of CuCl monomers with Brønsted acid sites, resulting in the formation of ZCu and the release of HCl. Cuprous oxide can form via the reaction of CuCl with traces of water present in the zeolite, a process that is most likely to occur when the exchange temperature is 673 K. As the exchange temperature is raised to 1023 K, the formation of Cu_2O clusters becomes negligible, as does the retention of occluded CuCl. When exchange is carried out at 1023 K, 90% of the Cu present in the zeolite is present as ZCu and 10% as CuCl dimers. The average Cu−O coordination number for the Cu^+ cation located at the charge-exchange sites is 2.7 and the Cu−O bond distance is 1.98 Å. No evidence is found for the dealumination of the MFI structure during SSIE at temperatures up to 1023 K. The results of this study suggest that complete exchange of the Brønsted acid protons in H-ZSM-5 for Cu^+ cations via SSIE using CuCl requires thorough dehydration of the zeolite, the use of anhydrous CuCl, and an SSIE temperature of 1023 K.

Acknowledgment. The synchrotron laboratories of SSRL and ALS are acknowledged for the allocated beamtime and assistance. This work was supported by the Methane Conversion Cooperative, funded by BP.

CM052291M

(54) Hargittai, M.; Schwerdtfeger, P.; Réffy, B.; Brown, R. *Chem. Eur. J.* **2003**, *9*, 327.